Hindawi
Geofluids
Volume 2022, Article ID 6193082, 11 pages
https://doi.org/10.1155/2022/6193082

Research Article

Experimental Study on the Oil Recovery Performance of CO_2 Huff-and-Puff Process in Fractured Tight Oil Reservoirs

Kun Qian,[1] **Yu Huang**,[2] **Yanfeng He**,[1] **Xiangji Dou**,[1] **and Xiaojun Wu**[1]

[1]*School of Petroleum Engineering, Changzhou University, Changzhou 213164, China*
[2]*Oil and Gas Production Engineering Service Center, Sinopec East China Oil and Gas Company, Taizhou, Jiangsu 225300, China*

Correspondence should be addressed to Kun Qian; qiankun@cczu.edu.cn

Received 14 January 2022; Accepted 11 February 2022; Published 2 March 2022

Academic Editor: Zheng Sun

In order to investigate energy supply capacity and oil production contribution of near-fracture and fracture-free zone in fractured tight oil reservoirs, a series of CO_2 huff-and-puff tests were designed and carried out in different experimental conditions. A fracture-matrix long-core system was established to simulate the near-fracture zone and matrix zone of tight oil reservoirs. The NMR technique was utilized to identify the microscopic remaining oil of certain core samples. The effects of fracture length, soaking time, depressurization method, and asphaltene precipitation on the oil recovery performance of CO_2 huff-and-puff process were evaluated, respectively. The results indicated that the dissolution and diffusion range of the injected CO_2 can be apparently increased from both macro and micro aspects through increasing the length or density of the fractures and extending the soaking time; and, during puff period, the slow depressurization method has better recovery effect on near-fracture zone, while the step depressurization method has better recovery effect on distal fracture-free matrix. After CO_2 huff-and-puff process, the oil recovery of the medium pores near fracture could be close to oil recovery of the large pores, which is higher than 60%. But, in the distal matrix, the oil recovery of the medium pores was only a little higher than depletion development. The remaining oil of medium pores in distal fracture-free matrix still has great potential to be developed after CO_2 huff-and-puff process.

1. Introduction

Tight oil has huge exploration and development potential [1] and the development of tight oil has become the key factor to the stable production of crude oil in China [2, 3]. In this study, the target reservoir is a typically tight oil reservoir located in Shanbei area, Northwest China. The average permeability of the formation is about 0.53 mD and the average porosity is only 8.3%. The production of tight oil reservoirs declines rapidly due to the limited supply capacity of the matrix, and the reservoir energy cannot be effectively replenished by conventional water injection due to the narrow pore throat [4, 5].

CO_2 injection has been proven to be an effective method to improve the oil recovery of tight oil reservoirs [6, 7]. Continuous CO_2 flooding, CO_2-WAG injection (water alternating gas injection), and CO_2 huff-and-puff process are commonly used CO_2-EOR (enhance oil recovery) techniques [7]. Due to great heterogeneity of the target tight oil reservoir, the continuous CO_2 flooding and CO_2-WAG injection could result in serious gas channeling and early breakthrough [8]. In consideration of these issues, CO_2 huff-and-puff process seems to be a feasible method to enhance oil recovery from tight oil reservoir.

Abedini and Torabi [9] and Pu et al. [10] investigated the oil recovery mechanisms and performance of the immiscible and miscible CO_2 huff-and-puff process, and it was found that interfacial tension reduction, oil swelling, and extraction of lighter components by CO_2, especially during miscible CO_2 injections, are the main oil recovery mechanisms during CO_2 huff-and-puff process. In comparison with conventional reservoirs, the effect of CO_2 diffusion and nanopore confinement plays a significant role in enhancing oil recovery of tight oil reservoirs [11–15]. Qian et al. [16] illustrated that CO_2 can enter small pores and extract the oil in the smaller and blind pores at higher injection pressure during CO_2 injection through nuclear magnetic resonance (NMR) technique. Zhang et al. [17] found that CO_2

molecular diffusion and capillary pressure lead to 3.8% increase of CO_2 huff-and-puff oil recovery performance in tight oil reservoirs through numerical model. For tight reservoirs with stronger heterogeneity and lower permeability, the CO_2 huff-and-puff technique can obtain higher incremental oil recovery factor on the base of depletion [18]. In addition, the production parameters in tight reservoirs have also been optimized through experimental and numerical simulations [5, 17, 19].

During the CO_2 huff-and-puff process in tight reservoirs, the presence of fractures is conducive to the entry of CO_2 into deep formation and increasing the exposure surface of tight matrix to CO_2 [20]. Wang [8] clarified the conductivity of fractures in tight oil reservoirs by the three-dimensional physical model with staged-fracturing horizontal well. Bai et al. [21] demonstrated that the fracture can increase the oil recovery of near-fracture zone by 14% compared with fracture-free zone. Additionally, fracture can significantly reduce the effect of matrix permeability on oil recovery of tight reservoirs. Also, the fracture filled with CO_2 can enlarge the interaction between CO_2 and the oil in matrix. Sun et al. [22] used the embedded discrete fracture model (EDFM) to conduct simulation of Middle Bakken tight oil reservoir and found that CO_2 diffusion is the most important factor of CO_2 huff-and-puff effectiveness on cumulative oil production.

In order to exploit the transport process of oil from matrix into the CO_2-filled factures system, Hawthorne et al. [20] conducted initial CO_2-exposure experiments and found that the hydrocarbons in very tight Bakken shale sample could be completely achieved with longer exposure time and smaller rock sizes. Further, Eide et al. [23] studied CO_2 diffusion in fractured chalk with X-Ray CT imagine during CO_2 injection process and found that the oil recovery by CO_2 diffusion is about 95% at core scale and the oil recovery by CO_2 diffusion is strongly influenced by system size. Wang demonstrated that when tight sandstone core plug is exposed to CO_2, the concentration-driven diffusion of hydrocarbons caused by CO_2 diffusion is the main mechanism to enhance oil recovery [24]. Wei et al. [25] utilized NMR technique to monitor the oil distribution in the matrix and fracture and indicated that the mass transfer between the matrix and fracture proceeded to increase oil production intensively during the soaking time in the first cycle and contributed less in second and third cycles. In addition, the characteristics of produced oil also indicated that the presence of fracture can increase the CO_2 mass transfer between CO_2 and oil in the matrix [26]. As mentioned, the CO_2 recovery mechanisms and effects on the oil recovery factor in fractured tight oil reservoirs have been widely studied; and the mass transfer between CO_2 and oil in the near-fracture matrix also has been discussed through CT, NMR, and oil composition analysis. However, the near-fracture tight formation was mainly investigated with the single-core samples exposed to CO_2. The energy supply capacity and microscopic remaining oil distribution of fracture-free matrix in fractured tight reservoirs during CO_2 huff-and-puff process need to be further characterized.

In this study, a fracture-matrix long-core system was firstly established to simulate the near-fracture zone and matrix zone of tight oil reservoirs. Then, a series of CO_2 huff-and-puff tests were designed and carried out in different experimental conditions. The NMR technique was utilized to identify the microscopic remaining oil of certain core samples. The effects of fracture length, soaking time, and depressurization method on the oil recovery performance were evaluated, respectively. Additionally, the permeability reduction was measured to determine the formation damage caused by asphaltene precipitation. The results of this study provide a further understanding of energy supply capacity of near-fracture and fracture-free zone during CO_2 huff-and-puff process. Meanwhile, the oil production contribution of different pores in fractured tight oil reservoirs was investigated.

2. Experimental Section

2.1. Fracture-Matrix Long-Core System. During the development process of tight oil reservoirs, the artificial fractures are developed near the well [5]. The fractured cores or matrix cores utilized in physical simulation alone cannot accurately characterize the fractured tight oil reservoirs. Therefore, the artificial fractured cores and matrix cores were combined to establish a fracture-matrix system to simulate fractured oil reservoirs, shown in Figure 1. Squeezing and pressing method was used to generate fractures. The rough wall surface of the fracture was covered with quartz sands. Then, the broken core was recombined and fixed with a heat shrinkable sleeve (Figure 2).

2.2. Materials. In this study, five tight sandstone core samples were collected from Chang 8 reservoir of Changqing Oil Field, China. Among them, core #1 and core #2 were artificially fractured. The properties of cores are listed in Table 1. The cores were composited to establish long core A and long core B with different fracture length (Figure 3).

The original oil sample and brine sample were also collected from Chang 8 reservoir. The density and viscosity of the oil sample were measured to be 843.4 kg/m^3 and 3.37 mPa s at the atmospheric pressure and the reservoir temperature of 61°C. The Gas Chromatography (GC) compositional analysis of the crude oil sample is shown in Figure 4 with Agilent 7890A chromatography. The purity of CO_2 used in this study was equal to 99.99% supplied by Beijing Huayuan Gas Chemical Co., Ltd. The minimum miscible pressure (MMP) between the crude oil and CO_2 was 22.33 MPa with slim-tube tests at reservoir temperature.

The reservoir brine sample was collected from the same formation and cleaned. The reservoir brine has the total dissolved solids (TDS) of 30917.8 mg/L, which was evaluated to be the water type of calcium chloride. The brine viscosity was measured to be 0.43 mPa s at the atmospheric pressure and 61°C.

2.3. Experimental Procedures of CO_2 Huff-and-Puff Tests. The experimental conditions of this study are shown in Table 2 and the experimental flow chart is shown in Figure 5. The general procedure of the CO_2 huff-and-puff tests is briefly described as follows:

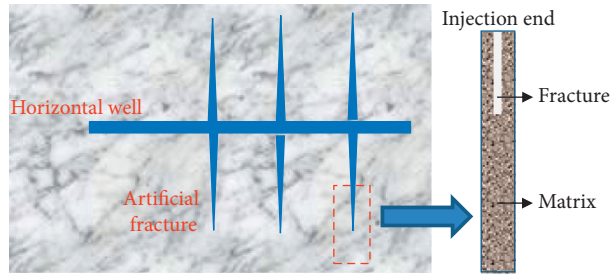

Figure 1: Diagram of fracture-matrix long-core system.

Figure 2: Artificial fractured core.

Table 1: Basic properties of core samples.

Core no.	Type	Length (cm)	Porosity (%)		Permeability (mD)	
			Before fracture	After fracture	Before fracture	After fracture
1	Fracture	5.014	11.86	12.35	1.56	1249.34
2	Fracture	5.776	11.40	11.74	1.94	896.21
3	Matrix	4.876	13.46	—	3.10	—
4	Matrix	5.028	13.61	—	3.02	—
5	Matrix	5.992	12.75	—	2.20	—

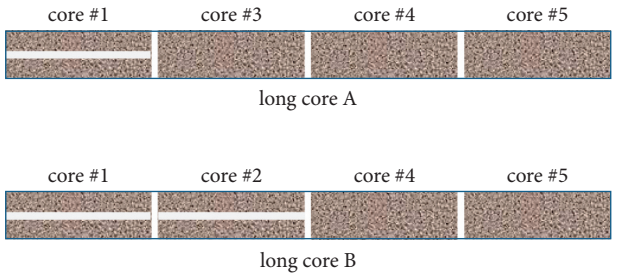

Figure 3: Schematic diagram of long core A and long core B.

(1) Prior to each test, the core plugs were thoroughly cleaned by using a Dean-Stark extractor (SXT-02, Shanghai Ping Xuan Scientific Instrument Co., Ltd.,

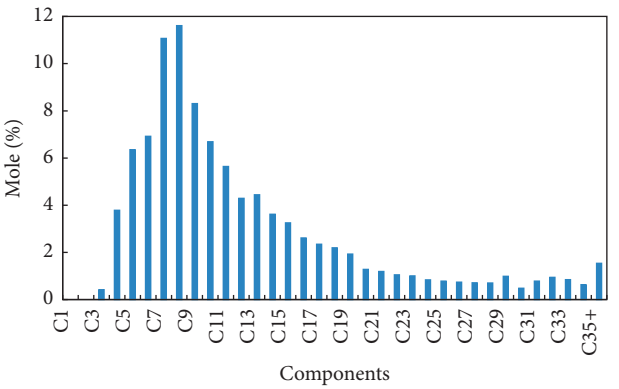

Figure 4: Components of the oil sample under the temperature of 21°C.

Table 2: Conditions of CO_2 huff-and-puff tests at the reservoir temperature of 61°C.

Test number	Long core number	Fracture length (cm)	Initial oil saturation (%)	Soaking time (h)	Pressure-drop method
1	A	5.014	63.25	12	Rapid
2	B	10.790	65.77	12	Rapid
3	A	5.014	65.93	24	Rapid
4	B	10.790	66.07	12	Slow
5	B	10.790	66.29	12	Step

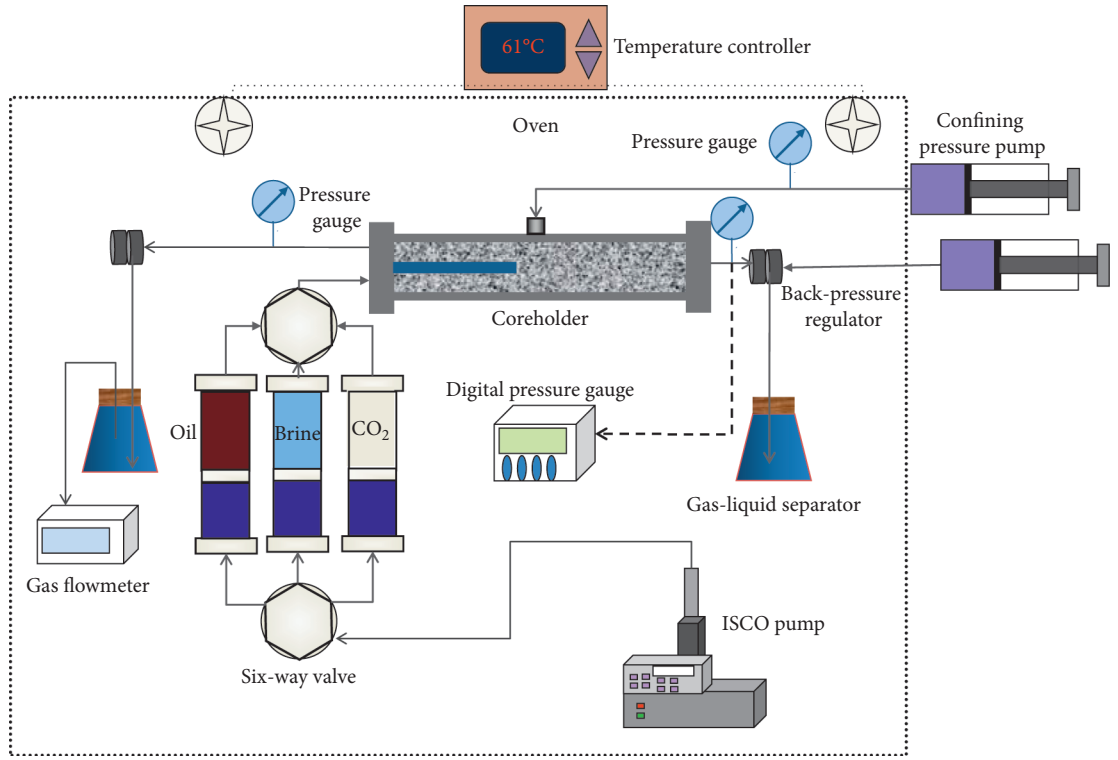

Figure 5: Schematic diagram of the experimental setup used for CO_2 huff-and-puff tests conducted at temperature of 61°C.

China) for 20~30 days. After the core plugs were cleaned and dried at 100°C, the gas permeability and porosity were measured with nitrogen (High-Pressure Gas Permeameter/Porosimeter, Temco, Tulsa, USA).

(2) The target core plugs were placed in core holder and vacuumed for 48 hours. The formation brine prepared with deuterium water was injected at the flow rate of 0.2 cm^3/min to saturate the core plugs, and the saturated cores were moved to NMR apparatus and scanned to make sure the hydrogen signal of the brine is eliminated. Then the core plugs were placed in the long-core holder again and displaced by brine again to ensure complete water saturation.

(3) After that, 3.0 PV of the crude oil was pumped through the core plug at a constant rate of 0.1 cm^3/min until no water was produced to achieve the connate water saturation (S_{wc}) and the initial oil saturation (S_{oi}) at the reservoir temperature of 61°C. The T_2 spectrum of the certain cores was measured again after the core plugs had been saturated with crude oil.

(4) The certain core plugs were placed in the long-core holder in order. The long core was displaced by crude oil again to ensure complete oil saturation. The long-core system was pressurized to the initial formation pressure of 20 MPa with crude oil. Afterwards, the depletion development was conducted to the atmospheric pressure by reducing back pressure.

(5) After depletion development, CO_2 was injected under constant pressure. After the distal end of the core holder reached the desired pressure of 16 MPa, which is the current formation pressure, the pump continued the constant pressure condition for 30 min and the soaking time was adjusted according to the experiment needs. The puff cycle was then started at the injection end of the core holder with

the pressure of atmosphere. These cycles were continued until no considerable oil production was obtained. The injection and production pressure was continuously monitored and recorded. The cumulative produced oil volume was recorded by a video camera and the cumulative volume of the produced gas was measured and recorded by using the gas flow meter.

(6) After the CO_2 huff-and-puff tests, the T_2 spectrum of the certain core samples was measured with NMR apparatus.

(7) Change the experimental conditions and repeat the above experimental steps.

3. Results and Discussion

3.1. Effects of Fracture Length. Long core A and long core B with different fracture length (Figure 3) were established to conduct CO_2 huff-and-puff tests. The oil recovery factors of long core A and long core B during depletion development are 12.62% and 13.43%, respectively. Long core B with longer fracture can obtain higher cumulative oil recovery factor with less huff-and-puff cycles. After the entire huff-and-puff tests, the ultimate recovery factor of long core B is 5.37% higher than that of long core A, which are, respectively, 51.14% and 45.77%, as shown in Figure 6.

Combined with the peak and trough in the T_2 spectrum, the matrix and fracture of the core can be identified in the initial oil-saturated state. The T_2 spectrum was artificially divided into three intervals [16], micro pores (≤5 ms), medium pores (5~100 ms), large pores, and fractures (≥100 ms). As shown in Figure 7, the remaining oil distributions of core #1 after the ultimate huff-and-puff tests with long core A and long core B are similar. But more oil in micro pores of core #1 was obtained in long core A (Figure 7), due to the one more huff-and-puff cycle in long core A. The oil recovery factors of core #1 after tests with long core A and long core B are 68.23% and 67.01%, respectively. In the near-fracture zone, the oil recovery factor of micro pores can be close to 20% and the lower oil recovery limit of pores can be as low as the pore radius corresponding to the T_2 relaxation time of 1 ms (Figure 7).

Core #3 was the matrix core closest to the fracture and core #5 was the furthest matrix core from the fracture in long core A. After huff-and-puff tests with long core A, the ultimate oil recovery factor of core #3 was 44.31% and the ultimate oil recovery factor of core #5 was only 14.79%. Obviously, with the distance from the fracture increasing, the effect of CO_2 huff-and-puff process becomes poorer. When the fracture was extended from long core A to long core B, the oil recovery of core #5 was significantly increased from 14.79% to 28.42%. Figure 8 presents that the increased production mainly comes from medium and large pores corresponding to the T_2 relaxation time more than 5 ms. The lower oil recovery limit of distal matrix can decrease with fracture extending. The extended fracture can not only expand oil drainage range but also improve the mass-transfer efficiency of CO_2. Therefore, higher oil recovery factor could be achieved with less huff-and-puff cycles through increasing the length or density of the fractures.

The distance from the matrix core plug center to the fracture is calculated and listed in Table 3. Figure 9 shows the oil recovery factor of different pores in matrix with different distances to the fracture. The farther away it is from the fracture, the lower the oil recovery is in different pores. As presented in Figure 9, the oil recovery factor of the oil in medium pores has the largest decline. In the near-fracture zone, the oil recovery of the medium pores could be close to the oil recovery of the large pores and fractures (Figure 9), which was higher than 60%. But, in the distal matrix, the cumulative oil recovery of the medium pores was 16.17%, which was only a little higher than oil recovery of depletion development.

In addition to large pores, the oil in medium pores could be the main force to production in Changqing tight oil reservoirs. CO_2 huff-and-puff technique only has a good effect on the oil recovery of near-fracture zone. But the remaining oil of medium pores in distal matrix still has great potential to be developed after CO_2 huff-and-puff process. Adjusting the CO_2 development method and changing the well pattern would be feasible methods to develop remaining oil in matrix [5, 12].

3.2. Effects of Soaking Time. Soaking time is a significant parameter in CO_2 huff-and-puff operation. The CO_2 huff-and-puff experiments with different soaking time were conducted with long core A. Figure 10 presents the difference between cumulative oil recovery factors of each huff-and-puff cycle with different soaking time of 12 h and 24 h. The cumulative recovery factor of soaking for 24 h with 3 cycles is slightly higher than that of soaking for 12 h with 6 cycles. It is beneficial for CO_2 to dissolve and diffuse in the oil with increasing the soaking time, especially for the tight reservoirs. For the same total soaking time of the whole CO_2 huff-and-puff process, longer soaking time with less cycles can have better recovery effect and save development cost. When the huff-and-puff tests continued to operate until no oil was produced, the cumulative recovery factor of soaking for 24 h was 8.42% higher than that of soaking for 12 h.

The remaining oil distribution of fractured core #1 and the distal matrix core #5 after the tests are shown in Figures 11 and 12. Microscopically, longer soaking time can increase the oil recovery factor of micro pores. The oil recovery factors of micro pores of core #1 and core #5 increased by 7.71% and 6.16%, respectively (Table 4). Meanwhile the lower oil recovery limit of pores decreased. The oil in smaller pores could be obtained with longer soaking time (Figures 11 and 12). Macroscopically, longer soaking time can increase CO_2 sweep efficiency. When the soaking time was 12 h, the recovery factor of core #5 was 14.79%. When the soaking time was increased to 24 h, the recovery factor of core #5 increased to 23.71%. Therefore, the dissolution and diffusion range of the injected CO_2 was apparently increased from both macro and micro aspects after extending soaking time.

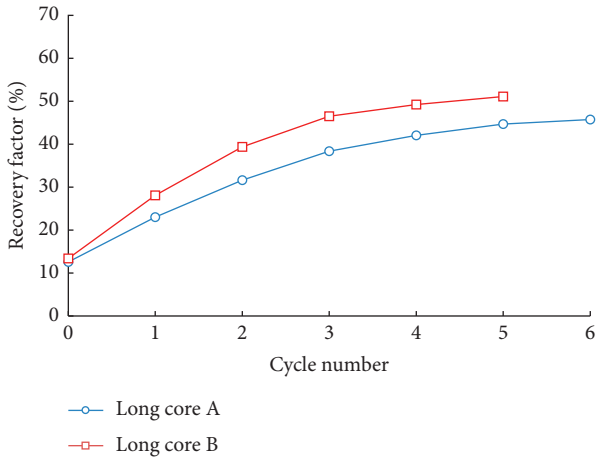

Figure 6: The difference between the cumulative oil recovery factors of long core A and long core B at each huff-and-puff cycle.

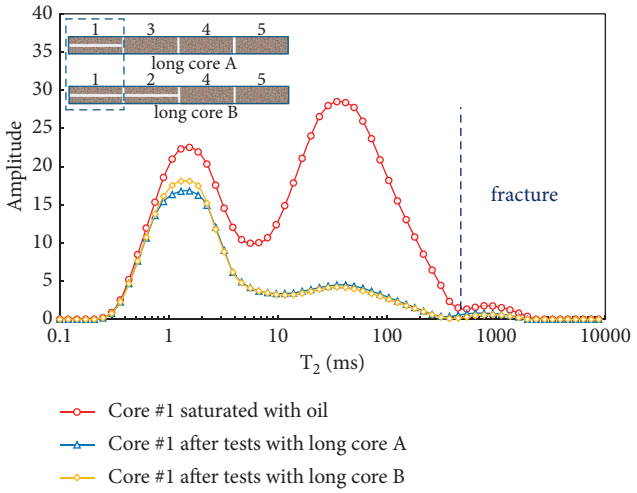

Figure 7: The difference between remaining oil distributions of core #1 after huff-and-puff tests with long core A and long core B.

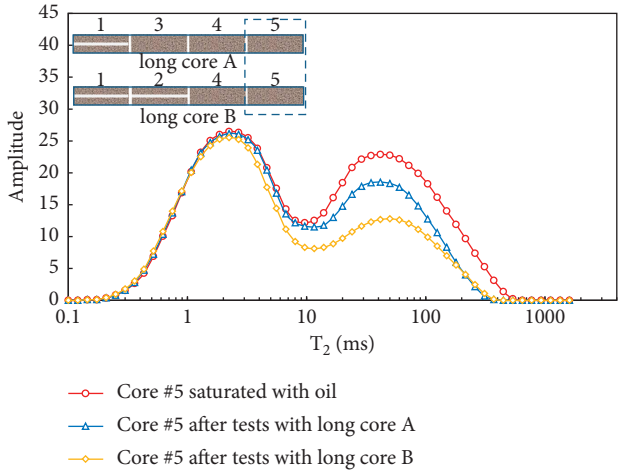

Figure 8: The difference between remaining oil distributions of core #5 after the huff-and-puff process with long core A and long core B.

Table 3: The distance from the core center to the fracture.

Core	The distance to the fracture (cm)	Oil recovery factor (%)
Core #1 in long core A	0	68.23
Core #1 in long core B	0	67.01
Core #3 in long core A	2.996	44.31
Core #5 in long core B	7.390	30.42
Core #5 in long core A	13.382	14.79

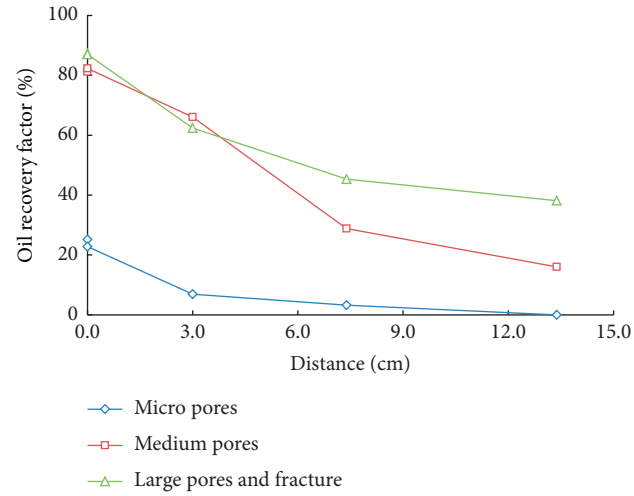

Figure 9: The oil recovery factor of different pores in matrix with different distances to the fracture.

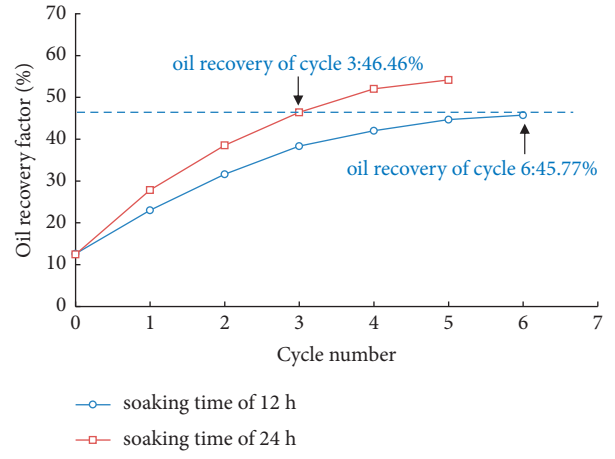

Figure 10: The difference between cumulative oil recovery factors of each huff-and-puff cycle with different soaking time.

3.3. Effects of Depressurization during Puff Period. In the puff period of the first huff-and-puff cycle, three different depressurization methods were performed. Table 5 presents the production status of different depressurization methods, and Figure 13 shows pressure change of distal end during different depressurization process.

According to production dynamics and oil recovery factor changing with time (Figure 14), the production period was divided into three stages:

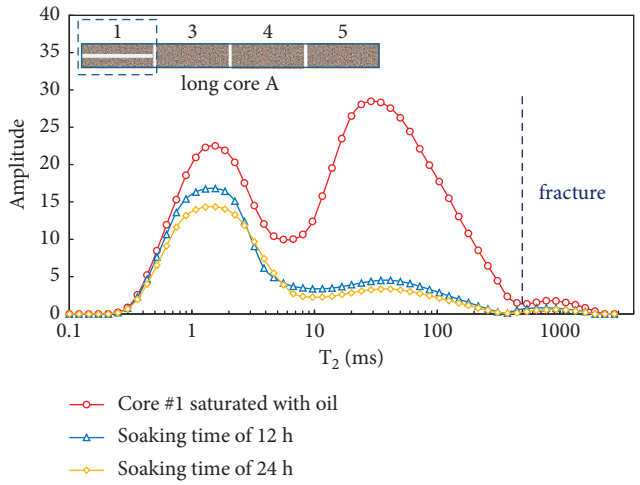

Figure 11: The microscopic remaining oil distribution of fractured core #1 after huff-and-puff tests with different soaking time.

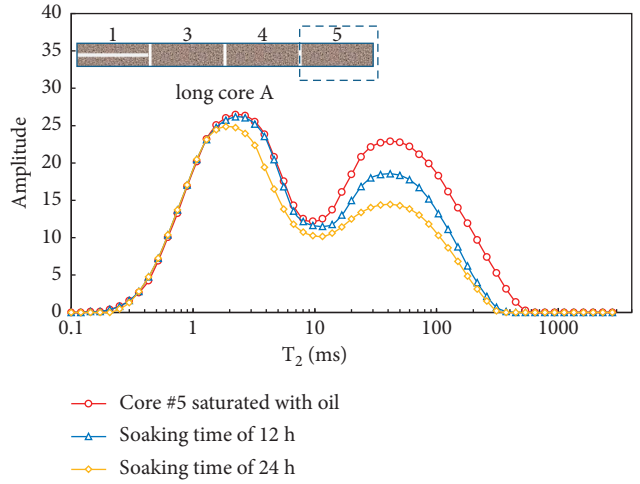

Figure 12: The microscopic remaining oil distribution of matrix core #5 after huff-and-puff tests with different soaking time.

Table 4: The oil recovery factor of different pores after huff-and-puff tests with different soaking time.

Core number	Pore types	Soaking time	
		12 h (%)	24 h (%)
Core #1	Micro pores (≤5 ms)	26.27	33.98
	Medium pores (5~100 ms)	82.12	87.14
	Large pores (≥100 ms)	87.13	90.50
	Total	68.23	70.92
Core #5	Micro pores (≤5 ms)	0.00	6.16
	Medium pores (5~100 ms)	16.00	31.33
	Large pores (≥100 ms)	47.13	59.46
	Total	14.79	23.71

(1) Gas flowback stage: in the huff period, the injected CO_2 preferentially occupied fractures and large pores and then dissolved and diffused into smaller pores [24]. After the soaking period, there was still a large amount of free gas remaining in the large pores and fractures. Therefore, at the beginning of each depressurization process, a large amount of gas was produced with the system pressure decreasing (Figure 13). This period was very short and there was almost no oil output (Figure 14(b)).

(2) Free gas drive stage: after CO_2 flowback, some free CO_2 was still trapped in the near-wellbore area. At the same time, there was also crude oil in the near-wellbore area and fractures. Then the oil was driven and carried out by free CO_2. At this stage, the oil and CO_2 were produced alternately, which was mainly manifested as a large section of gas and a small section of oil. The GOR (gas oil ratio) fluctuated greatly (Figure 15) and the oil production rate was relatively low (Figure 14(b)).

(3) Solution gas drive stage: during the depressurization process, dissolved gas was continuously released. When the oil production rate was significantly increased, the drive mode was changed from free gas drive to solution gas drive. When the solution gas drive proceeded to the final stage, the capacity of energy supply decreased. Solution gas drive stage was the main oil production stage in different depressurization method.

The cumulative oil recovery factor of puff period was influenced by the depressurization method (Figure 14(a)). After first cycle, the oil recovery factor of slow depressurization was 17.24%, which was higher than that of rapid depressurization process by 2.59%. Once the pressure started to drop, the CO_2 bubble began to nucleate. Then, the bubble grew and filled pores with the pressure decreasing [27]. In rapid depressurization process, the nucleated CO_2 bubbles were produced before they became larger to occupy the pore space due to the huge pressure gradient. So the crude oil in the pores could not be driven effectively by the dissolved gas. However, in slow depressurization process, the CO_2 nucleation had more time to grow to fill the pore space [28]. The grown CO_2 bubble can drive the crude oil in the matrix to the fracture and near-wellbore zone. When the CO_2 bubbles increased to a certain size, the narrow pore throat would hinder the mobility of the bubbles due to Jamin effect [29]. As pressure decreased, the gas bubbles could coalesce into a continuous gas phase and migrated. The GOR oscillated down during the first half of solution gas drive stage in the slow depressurization method.

The highest oil recovery factor of the three depressurization methods was step depressurization, which was 18.40%. There was little difference in production times between slow depressurization method and step depressurization method. But the step pressure-drop process can avoid the rapid fracture closure and the compression of pores due to the stress sensibility. So the oil in distal core could be recovered more smoothly. The highest oil recovery factor of step depressurization method illustrates that fracture closure time has great influence on the oil recovery of fractured tight sandstone reservoirs.

Figures 16 and 17 are the microscopic remaining oil distributions of fractured core #2 and distal matrix core #5 after huff-and-puff tests with different depressurization method. After injection, CO_2 preferentially entered the

Table 5: Production status of different depressurization methods.

Depressurization method	Back pressure (MPa) (production pressure)	Production valve (throttle valve)	Oil recovery factor of depletion (%)	Oil recovery factor of first cycle (%)
Rapid	0	50% open	13.43	14.65
Slow	0	10% open	13.29	17.24
Step	16-12-8-4-0	50% open	13.40	18.40

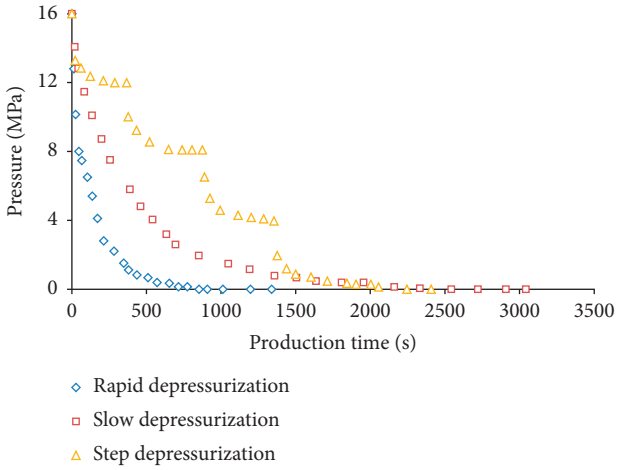

Figure 13: Pressure change of distal end during puff period of the first huff-and-puff cycle with different depressurization method.

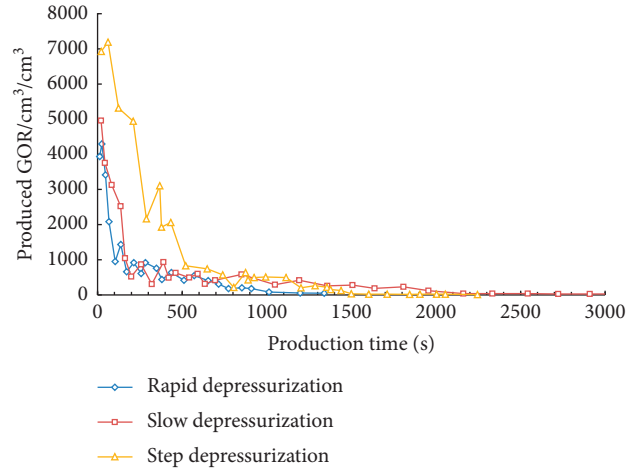

Figure 15: GOR during puff period of the first huff-and-puff cycle with different depressurization method.

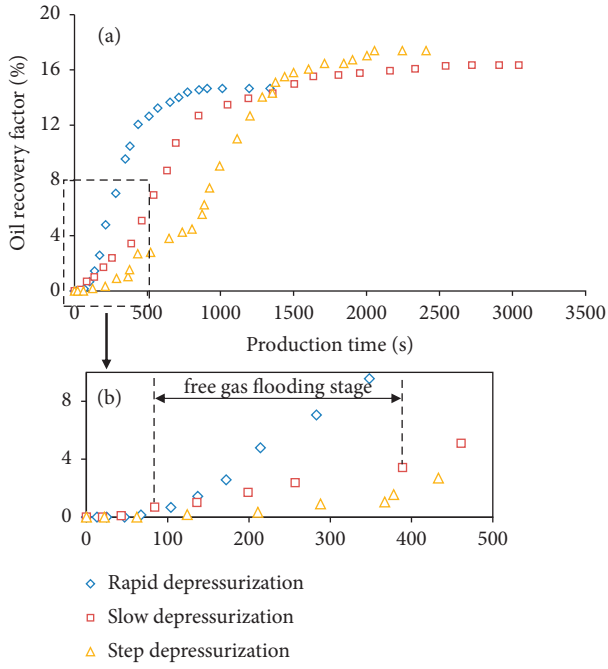

Figure 14: Oil recovery factor during puff period of the first huff-and-puff cycle with different depressurization method.

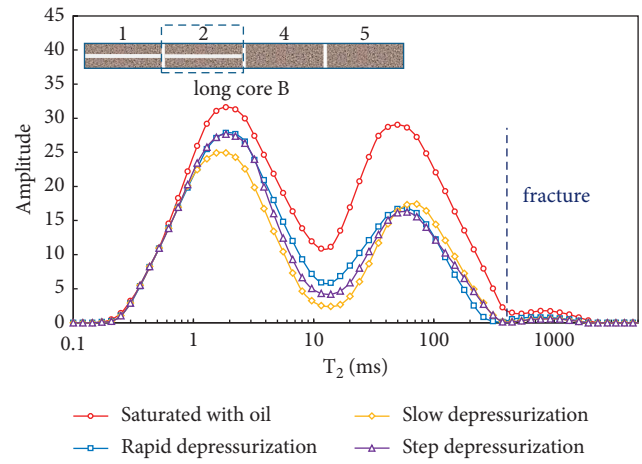

Figure 16: The microscopic remaining oil distribution of fractured core #2 after huff-and-puff tests with different depressurization method.

larger pores, dissolved, and diffused into the oil in micro pores [30]. The existence of fracture increased the dissolution and diffusion of CO_2 into the matrix with expanding the contact range between CO_2 and oil. Thus the oil recovery factor of the fractured core #2 was much higher than that of matrix core #5. Moreover, the oil recovery factor in pores of different sizes was overall higher in in near-fracture zone (Table 6).

In addition, the microscopic remaining oil distribution can also reflect the influence of different depressurization method on oil recovery (Figures 16 and 17). In near-fracture zone, both medium pores and large pores were the main contributors to oil production. The oil recovery factors of medium pores and large pores were around 50% (Table 6). In particular, in the solution gas drive stage of slow depressurization process, the CO_2 nucleation had more time to grow to drive the oil in the pores. Consequently, in fractured core #2, the oil recovery of the micro and medium pores is

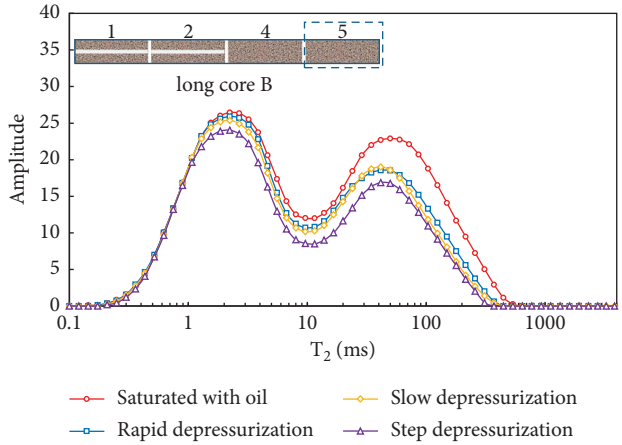

Figure 17: The microscopic remaining oil distribution of matrix core #5 after huff-and-puff tests with different depressurization method.

Table 6: The oil recovery factor of different pores after huff-and-puff tests with different depressurization method.

Pore types	Fractured core #2			Matrix core #5		
	Rapid (%)	Slow (%)	Step (%)	Rapid (%)	Slow (%)	Step (%)
Micro pores (≤5 ms)	11.93	20.50	13.02	2.13	4.76	9.83
Medium pores (5~100 ms)	45.78	55.75	51.35	15.80	17.98	28.94
Large pores (≥100 ms)	60.36	48.07	53.07	38.40	48.81	55.22
Total	36.16	39.37	37.29	18.67	19.17	23.85

higher than rapid and step depressurization methods (Figure 16, Table 6). But the oil recovery of the large pores in slow depressurization was less than the other two methods, because part of the oil from the micro and medium pores was retained in the large pores in the last stage of slow depressurization method with low pressure difference.

In matrix core #5, the microscopic remaining oil distributions of the rapid and slow depressurization methods are much the same (Figure 17 and Table 6). The microscopic remaining oil distribution of the step depressurization method is obviously lower than those of the other two methods, and the oil in smaller pores can be recovered (Figure 17). During the process of step depressurization process, the fracture closure time was postponed, which is conductive to the oil drainage from matrix to fracture.

After the entire huff-and-puff cycles, the oil recovery factors of the huff-and-puff process with rapid, slow, and step depressurization were 51.14%, 53.28%, and 55.54%, respectively. The oil recovery factor of the first huff-and-puff cycle is obviously different, as presented in Figure 18. With cycles proceeding, the remaining oil saturation decreased and the remaining oil viscosity increased [31]. The solubility of CO_2 in the remaining oil was also getting less. The advantage of the slow depressurization method in solution gas drive stage decreased. For this reason, the oil recovery factor of slow depressurization method became closer to that of fast depressurization method in each cycle. As mentioned before, the oil recovery factor of huff-and-puff process with step depressurization process was always higher. Therefore, step depressurization combined with slow pressure drop during puff period in the first two cycles is an effective method to increase the oil recovery factor of the CO_2 huff-and-puff process of tight oil reservoirs. In the later cycles, the depressurization combined with rapid pressure drop can be utilized to save production time.

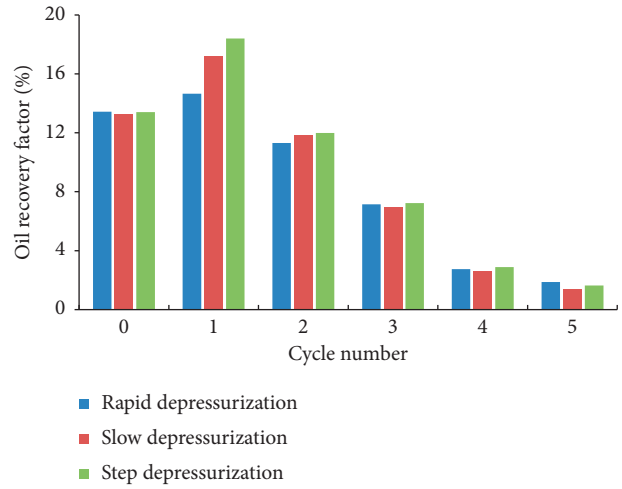

Figure 18: The oil recovery factor of depletion production period and each huff-and-puff cycle with different depressurization method.

3.4. Effects of Asphaltene Precipitation. After the CO_2 huff-and-puff process with long core A of Test 1, the core samples were cleaned by a Soxhlet Extractor with the solvent of petroleum ether which cannot dissolve asphaltene [32]. The percentage of permeability reduction is obtained by comparing the gas permeability of the core before and after CO_2

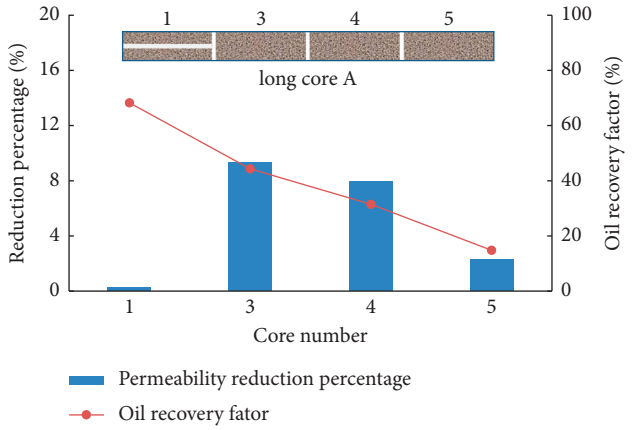

Figure 19: Permeability reduction percentage and oil recovery factor of different cores in long core A.

huff-and-puff tests, which is calculated by the following equation:

$$R_k = \frac{K_{gb-}K_{ga}}{K_{gb}} \times 100\%, \quad (1)$$

where R_k is the permeability reduction percentage of the core sample, %; K_{gb} is the gas permeability of the core sample before CO_2 flooding, mD; K_{ga} is the gas permeability of the core sample after CO_2 flooding, mD.

The injected CO_2 destroys the stable state of the asphaltene-resin system, which leads to the flocculation and precipitation of the asphaltene [9]. In the CO_2 huff-and-puff tests, asphaltene precipitation still occurred [16] and the permeability of the cores decreased after the huff-and-puff tests in tight oil reservoirs. The asphaltene particles were difficult to be transported out because of the small pore throats of the matrix. But the asphaltene precipitation had little effects on the permeability of fractured core #1 with strong flow conductivity. As shown in Figure 19, the permeability reduction percentage has a certain positive correlation with oil recovery factor, except fractured core #1, because, in the CO_2 huff-and-puff process, the higher oil recovery factor indicates the better solubility of CO_2 in oil. The permeability reduction percentages of core #3 and core #4 are 12.20% and 9.93%, respectively, while the permeability reduction percentage of distal core #5 is only 3.64% due to the lowest CO_2 solubility.

4. Conclusions

In this paper, a series of CO_2 huff-and-puff tests were conducted with fractured tight cores from Changqing Oil Field, China. The NMR technique was utilized to analyze the remaining oil of the core plugs. The effects of fracture length, soaking time, depressurization method, and asphaltene precipitation on the oil recovery performance were evaluated. According to the obtained experimental results, the following conclusions have been drawn:

(1) Higher oil recovery factor could be achieved with less huff-and-puff cycles through increasing the length or density of the fractures and extending the soaking time. Moreover, the dissolution and diffusion range of the injected CO_2 could be apparently increased from both macro- and microaspects.

(2) In addition to large pores, the remaining oil of medium pores in distal fracture-free matrix still has great potential to be developed after CO_2 huff-and-puff process. Adjusting the CO_2 development method and changing the well pattern would be feasible methods to develop remaining oil.

(3) Step depressurization combined with slow pressure drop during puff period in the first two cycles is an effective method to increase the oil recovery factor of the CO_2 huff-and-puff process of tight oil reservoirs. In the later cycles, the depressurization combined with rapid pressure drop can be utilized to save production time.

(4) During CO_2 huff-and-puff process, the asphaltene precipitation has little effects on the permeability of the near-fracture zone. But the matrix closer to the injection end has more serious asphaltene precipitation and greater permeability loss than distal matrix.

Data Availability

The data used to support the findings of this study are available from the corresponding author upon request.

Conflicts of Interest

The authors declare that they have no conflicts of interest.

Acknowledgments

This research was supported by the National Natural Science Foundation of China (funding name: Study on the Microscopic Phase Behavior and Migration Mechanism of CO_2 and Multicomponent Alkanes in Shale Dynamical Nanopore) (no. 52004038) and CNPC-CZU Innovation Alliance Funding (funding name: Development of Multi-Component Thermofluid Experimental Equipment and Research on the Mechanism of Multi-Component Thermofluid).

References

[1] N. Zhou, S. Lu, and M. Wang, "Limits and grading evaluation criteria continental basins of China," *Petroleum Exploration and Development*, vol. 48, no. 5, pp. 939–949, 2021.

[2] C. Jia, C. Zou, J. Li, D. Li, and M. Zheng, "Evaluation criteria, major types, characteristics and resource prospects of tight oil in China," *Petroleum Research*, vol. 1, no. 1, pp. 1–9, 2016.

[3] L. Sun, C. Zou, A. Jia et al., "Development characteristics and orientation of tight oil and gas in China," *Petroleum Exploration and Development*, vol. 46, no. 6, pp. 1073–1087, 2019.

[4] Y. Tang, R. Wang, Z. Li, M. Cui, Z. Lun, and Y. Lu, "Experimental study on spontaneous imbibition of CO_2-rich brine in tight oil reservoirs," *Energy & Fuels*, vol. 33, no. 8, pp. 7604–7613, 2019.

[5] P. Zuloaga, W. Yu, J. Miao, and K. Sepehrnoori, "Performance evaluation of CO_2 huff-n-puff and continuous CO_2 injection in tight oil reservoirs," *Energy*, vol. 134, pp. 181–192, 2017.

[6] A. K. Al-Khazraji and M. B. Awang, "Evaluation of miscible CO_2-flooding to improve oil recovery in a clastic heterogeneous reservoir," in *Proceedings of the IADC/SPE Asia Pacific Drilling Technology Conference*, Singapore, August 2016.

[7] Z. Song, Y. Song, Y. Li, B. Bai, K. Song, and J. Hou, "A critical review of CO_2 enhanced oil recovery in tight oil reservoirs of north America and China," *Fuel*, vol. 276, no. 5, Article ID 118006, 2020.

[8] W. Xue-wu, X. Pufu, Y. Zheng-ming, L. Xue-wei, X. Zhi-zeng, and W. Li-qiang, "Laboratory and field-scale parameter optimization of CO_2 huff-n-puff with the staged-fracturing horizontal well in tight oil reservoirs," *Journal of Petroleum Science and Engineering*, vol. 186, Article ID 106703, 2020.

[9] A. Abedini and F. Torabi, "Oil recovery performance of immiscible and miscible CO_2 huff-and-puff processes," *Energy & Fuels*, vol. 28, no. 2, pp. 774–784, 2014.

[10] W. Pu, B. Wei, F. Jin et al., "Experimental investigation of CO_2 huff-n-puff process for enhancing oil recovery in tight reservoirs," *Chemical Engineering Research and Design*, vol. 111, pp. 269–276, 2016.

[11] A. Habibi, M. R. Yassin, H. Dehghanpour, and D. Bryan, "Experimental investigation of CO_2-oil interactions in tight rocks: a montney case study," *Fuel*, vol. 203, pp. 853–867, 2017.

[12] J. J. Sheng and B. L. Herd, "Critical review of field EOR projects in shale and tight reservoirs," *Journal of Petroleum Science and Engineering*, vol. 159, pp. 654–665, 2017.

[13] D. Alfarge, M. Wei, B. Bai, and A. Almansour, "Effect of molecular-diffusion mechanisim on CO_2 huff-n-puff process in shale-oil reservoirs," in *Proceedings of the SPE Kingdom of Saudi Arabia Annual Technical Symposium and Exhibition*, Dammam, Saudi Arabia, April 2017.

[14] Z. Sun, B. Huang, Y. Li, H. Lin, S. Shi, and W. Yu, "Nanoconfined methane flow behavior through realistic organic shale matrix under displacement pressure: a molecular simulation investigation," *Journal of Petroleum Exploration and Production Technology*, vol. 335, pp. 1–9, 2021.

[15] Z. Sun, B. Huang, K. Wu et al., "Nanoconfined methane density over pressure and temperature: wettability effect," *Journal of Natural Gas Science and Engineering*, vol. 99, Article ID 104426, 2022.

[16] K. Qian, S. Yang, H. Dou, Q. Wang, L. Wang, and Y. Huang, "Experimental investigation on microscopic residual oil distribution during CO_2 huff-and-puff process in tight oil reservoirs," *Energies*, vol. 11, no. 10, p. 2843, 2018.

[17] Y. Zhang, W. Yu, Z. Li, and K. Sepehrnoori, "Simulation study of factors affecting CO_2 huff-n-puff process in tight oil reservoirs," *Journal of Petroleum Science and Engineering*, vol. 163, pp. 264–269, 2018.

[18] W. Yu, H. R. Lashgari, K. Wu, and K. Sepehrnoori, "CO_2 injection for enhanced oil recovery in bakken tight oil reservoirs," *Fuel*, vol. 159, pp. 354–363, 2015.

[19] Z. Lei, S. Wu, T. Yu et al., "simulation and optimization of CO_2 huff-n-puff processes in tight oil reservoir: a case study of chang-7 tight oil reservoirs in ordos basin," in *Proceedings of the SPE Asia Pacific Oil and Gas Conference and Exhibition*, Brisbane, Australia, October 2018.

[20] S. B. Hawthorne, C. D. Gorecki, J. A. Sorensen, E. N. Steadman, J. A. Harju, and S. Melzer, "Hydrocarbon mobilization mechanisms from upper, middle, and lower bakken reservoir rocks exposed to CO_2," in *Proceedings of the SPE Unconventional Resources Conference Canada*, Calgary, Canada, November 2013.

[21] H. Bai, Q. Zhang, Z. Li et al., "Effect of fracture on production characteristics and oil distribution during CO_2 huff-n-puff under tight and low-permeability conditions," *Fuel*, vol. 246, pp. 117–125, 2019.

[22] R. Sun, W. Yu, F. Xu, H. Pu, and J. Miao, "Compositional simulation of CO_2 huff-n-puff process in middle bakken tight oil reservoirs with hydraulic fractures," *Fuel*, vol. 236, pp. 1446–1457, 2019.

[23] Ø. Eide, M. A. Fernø, Z. Alcorn, and A. Graue, "Visualization of carbon dioxide enhanced oil recovery by diffusion in fractured chalk," *SPE Journal*, vol. 21, no. 1, pp. 112–120, 2016.

[24] H. Wang, Z. Lun, C. Lv et al., "Nuclear-magnetic-resonance study on mechanisms of oil mobilization in tight sandstone reservoir exposed to carbon dioxide," *SPE Journal*, vol. 23, no. 3, pp. 750–761, 2018.

[25] B. Wei, K. Gao, T. Song et al., "Nuclear-magnetic-resonance monitoring of mass exchange in a low-permeability matrix/fracture model during CO_2 cyclic injection: a mechanistic study," *SPE Journal*, vol. 25, no. 1, pp. 440–450, 2020.

[26] B. Wei, M. Zhong, K. Gao et al., "Oil recovery and compositional change of CO_2 huff-n-puff and continuous injection modes in a variety of dual-permeability tight matrix-fracture models," *Fuel*, vol. 276, Article ID 117939, 2020.

[27] D. S. George, O. Hayat, and A. R. Kovscek, "A microvisual study of solution-gas-drive mechanisms in viscous oils," *Journal of Petroleum Science and Engineering*, vol. 46, no. 1-2, pp. 101–119, 2005.

[28] P. Nguyen, J. W. Carey, H. S. Viswanathan, and M. Porter, "Effectiveness of supercritical-CO_2 and N_2 huff-and-puff methods of enhanced oil recovery in shale fracture networks using microfluidic experiments," *Applied Energy*, vol. 230, pp. 160–174, 2018.

[29] M. Zhang, Q. Sang, H. Gong, Y. Li, and M. Dong, "Effect of depletion rate on solution gas drive in shale," *IOP Conference Series: Earth and Environmental Science*, vol. 108, no. 3, Article ID 032078, 2018.

[30] H. Gao, Y. Liu, Z. Zhang, B. Niu, and H. Li, "Impact of secondary and tertiary floods on microscopic residual oil distribution in medium-to-high permeability cores with NMR technique," *Energy & Fuels*, vol. 29, no. 8, pp. 4721–4729, 2015.

[31] M. Cao and Y. Gu, "Physicochemical characterization of produced oils and gases in immiscible and miscible CO_2 flooding processes," *Energy & Fuels*, vol. 27, no. 1, pp. 440–453, 2013.

[32] E. Y. Sheu, "Petroleum asphaltene properties, characterization, and issues," *Energy & Fuels*, vol. 16, no. 1, pp. 74–82, 2002.